Partially flexible MEMS neural probe composed of polyimide and sucrose gel for reducing brain damage during and after implantation

OPEN ACCESS
IOP Publishing
Journal of Micromechanics and Microengineering
J. Micromech. Microeng. **24** (2014) 025010 (10pp)
doi:10.1088/0960-1317/24/2/025010

Partially flexible MEMS neural probe composed of polyimide and sucrose gel for reducing brain damage during and after implantation

Myounggun Jeon[1,2], Jeiwon Cho[3], Yun Kyung Kim[4], Dahee Jung[3], Eui-Sung Yoon[1], Sehyun Shin[2] and Il-Joo Cho[1,5]

[1] Center for BioMicrosystems, Korea Institute of Science and Technology, Seoul, Korea
[2] School of Mechanical Engineering, Korea University, Seoul, Korea
[3] Center for Neuroscience, Korea Institute of Science and Technology, Seoul, Korea
[4] Center for Neuro-Medicine, Korea Institute of Science and Technology, Seoul, Korea

E-mail: ijcho@kist.re.kr

Received 22 August 2013, revised 18 November 2013
Accepted for publication 22 November 2013
Published 10 January 2014

Abstract

This paper presents a flexible microelectromechanical systems (MEMS) neural probe that minimizes neuron damage and immune response, suitable for chronic recording applications. MEMS neural probes with various features such as high electrode densities have been actively investigated for neuron stimulation and recording to study brain functions. However, successful recording of neural signals in chronic application using rigid silicon probes still remains challenging because of cell death and macrophages accumulated around the electrodes over time from continuous brain movement. Thus, in this paper, we propose a new flexible MEMS neural probe that consists of two segments: a polyimide-based, flexible segment for connection and a rigid segment composed of thin silicon for insertion. While the flexible connection segment is designed to reduce the long-term chronic neuron damage, the thin insertion segment is designed to minimize the brain damage during the insertion process. The proposed flexible neural probe was successfully fabricated using the MEMS process on a silicon on insulator wafer. For a successful insertion, a biodegradable sucrose gel is coated on the flexible segment to temporarily increase the probe stiffness to prevent buckling. After the insertion, the sucrose gel dissolves inside the brain exposing the polyimide probe. By performing an insertion test, we confirm that the flexible probe has enough stiffness. In addition, by monitoring immune responses and brain histology, we successfully demonstrate that the proposed flexible neural probe incurs fivefold less neural damage than that incurred by a conventional silicon neural probe. Therefore, the presented flexible neural probe is a promising candidate for recording stable neural signals for long-time chronic applications.

Keywords: flexible probe, MEMS neural probe, neuron damage, polyimide, sucrose gel

(Some figures may appear in colour only in the online journal)

[5] Author to whom any correspondence should be addressed.

1. Introduction

Understanding of the nervous system and brain functions has been one of the most important issues in neuroscience and neural rehabilitation [1–6]. Thus, many research groups have analyzed neural signals in the brain using implantable prostheses such as wire electrodes and neural probes [3, 5, 7]. By using these tools, they recorded single neuron spike signals by stimulating neurons at specific regions of the brain to study their corresponding functions [8, 9]. Analysis of these neural spikes from stimulated neurons at specific regions enables neuroscientists to discover specifics of brain functions of those regions. Also, these methods help us to find the causes of brain disease such as Parkinson's disease, epilepsy and chronic pains by analyzing lack of brain functions through stimulating neurons and recording neural spikes [10, 11].

The first implantable microelectrodes to record electrical activities in the extracellular environments were introduced in the 1950s. These microwires composed of tungsten [12] or stainless steel [13] were coated with an insulation layer except at the tip for recording of neural signals. The microwires composed of two or four electrodes (stereotrode or tetrode, respectively) have been further developed to record and sort neural spike signals of individual neurons [14]. However, a further increase in the number of electrodes of these microwires is difficult while the demands for massive parallel recording is continuously increasing to capture more neural signals at a time and to study correlations between different brain regions [15–17]. In addition, not only it is difficult to accurately implant microwires in different regions of the brain at a time, but also microwires may induce large neuron damages during the insertion processes.

To overcome these limitations and achieve a massive parallel neural signal recording, microelectromechanical systems (MEMS) neural probes have been introduced. MEMS technology has enabled the integration of a high-density microelectrode array on a planar silicon shank structure to stimulate neurons and record neural signals [18–24]. A small mechanical structure reduces neuron damage during the insertion and the higher electrode density increases the possibility of recording neural signals. Also, a precisely defined distance between multiple probe shanks allows recording of neural signals in different brain regions and investigating the functional connectivity between these regions. Among these MEMS neural probes, 'Michigan probe' [25–29] and 'Utah probe' [30–33] are most widely used. While the Michigan probe consists of multiple microelectrodes located on the probe surface, the Utah probe consists of a single electrode at the end of each silicon shank. In addition to these MEMS probes for electrical stimulation and recording, various multifunctional MEMS neural probes have been introduced such as drug delivery probes [25] and probes integrated with optical stimulation capability [34, 35]. However, most MEMS neural probes are made up of silicon which suffer from the mechanical mismatch between the stiff silicon and the soft brain tissue [36]. Therefore, when the rigid silicon probe is used to record the neural signal for a long time, the soft tissues are damaged due to the micro-motions of a brain. In addition, the immune responses cause macrophage to accumulate around the silicon probe. In summary, long-term chronic neural signal recording is challenging because either neural spikes of interest are no longer available due to cell death or the macrophages physically block the electrodes from the neural signals [37, 38].

Several methods have been proposed to reduce neuron damage and formation of macrophages. One of these trials is to use flexible MEMS neural probes. Flexible neural probes can reduce the immune responses because the flexible inserted structure can move with the brain movement. This flexible structure can be implemented with flexible polymer materials such as parylene [37], polyimide and SU-8 [39]. However, the flexible polymer probes are inevitably thicker than the conventional silicon probes to attain enough strength to be inserted into a brain. Thus, while the polymer materials help us to reduce chronic neuron damage after the insertion, the thick structure induces larger neuron damages during the insertion process. For example, several biodegradable materials have been coated on the flexible probes to enhance the stiffness during the insertion and maintain the flexibility after the insertion. Polyethylene glycol [40], silk-I protein polymer [41] and carboxy-methylcellulose [42] have been successfully used as biodegradable materials to enhance the probe stiffness and prevent buckling during the insertion. In addition to the larger damage incurred by the thick probes during the insertion, the probes coated with biodegradable materials must be inserted over a given time as the stiffness of materials starts to decrease when the probe contacts the wet brain tissues.

In this paper, a new flexible neural probe for chronic applications has been proposed with a goal to reduce neural damage both during and after the insertion process. Figure 1 shows the schematic diagram of the proposed flexible probe. The proposed flexible probe is composed of a rigid insertion segment and a flexible connection segment. The insertion segment is made of a thin rigid silicon structure to reduce neuron damages during the insertion process. In this proposed structure, this insertion segment is connected to the remaining body part anchored outside of the brain via a flexible polyimide. Therefore, the insertion segment can move according to brain movement, which reduces the brain damage after the probe is inserted as shown in figure 1(*b*). In the practical long-term chronic applications, the body of the probe is preferred to be mounted on the mouse head by bending the flexible segment 90° as shown in figure 1(*c*). To increase the stiffness of this probe to allow successful insertion into a brain, a biodegradable sucrose gel is selectively coated on the flexible polyimide. This sucrose gel increases the thickness of the probe, but does not induce neuron damage because it is designed to be located between the skull and brain surfaces.

This partially flexible structure can not only reduce brain damage during insertion due to the thin structure but also reduce brain damage after insertion due to the flexible connection segment. In addition, the insertion time of the proposed structure is not limited by the degradation time of the biodegradable polymer.

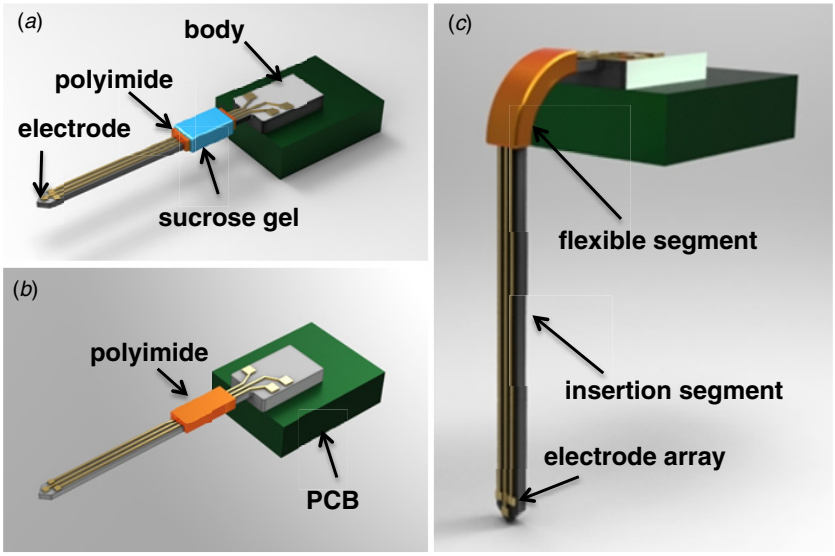

Figure 1. Schematic diagram of the proposed flexible MEMS neural probe. The probe has a flexible silicon shank and flexible connection: (*a*) the flexible neural probe coated with sucrose gel before implantation, (*b*) the neural probe with only flexible connection segment after sucrose gel is dissolved, (*c*) flexible status of the probe after implantation for long-term chronic applications.

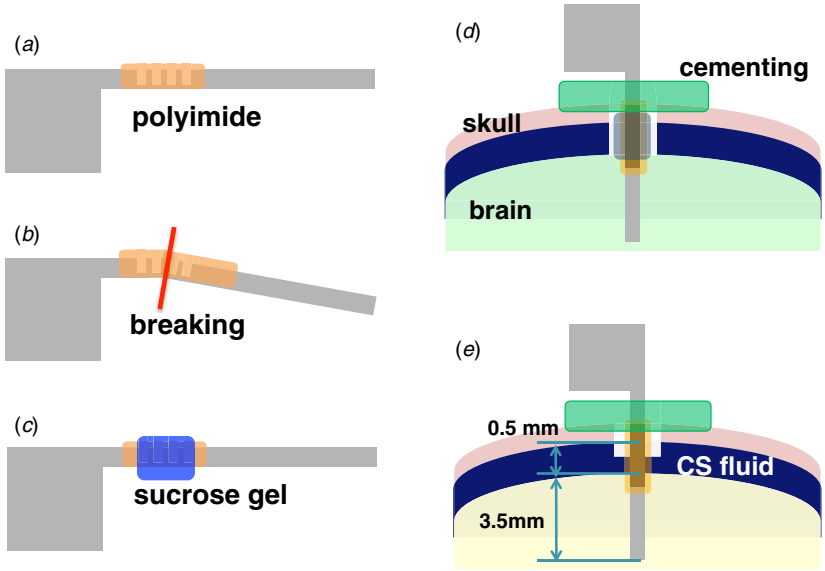

Figure 2. The concept and working principle of the flexible probe and *in vivo* implantation procedure. (*a*) The initial state of the flexible probe. (*b*) Breaking the silicon segment coated with the flexible polyimide. (*c*) Solidifying the flexible segment with the sucrose gel. (*d*) Implantation of the flexible neural probe in the brain. (*e*) Dissolution of the sucrose gel by the CSF between the skull and cortex.

2. Materials and methods

2.1. Design

In the proposed design, the flexible MEMS neural probe is composed of two segments: insertion segment and flexible connection segment. Figure 2 shows the working principle of the proposed flexible probe. Similar to that of the conventional silicon probes, the initial status of the flexible probe (i.e. as-fabricated probe) is not flexible as shown in figure 2(*a*). As opposed to the conventional silicon probe, the proposed probe consists of a flexible segment that is composed of an easily breakable silicon structure coated with a flexible polyimide. By breaking this silicon structure prior to the insertion, the probe that was initially rigid becomes flexible as shown in figure 2(*b*). The lattice silicon structure is used to define the breakable silicon structure to allow easy breaking of the probe by exerting a small force at the end of the probe. The flexible polyimide surrounding the broken silicon structure now connects the insertion segment of the probe to the remaining segment of the probe. However, to enhance the stiffness of the overall probe shank for successful insertion into the brain without buckling, the flexible region is further coated with a biodegradable material (4% sucrose gel) (figure 2(*c*)). The flexible segment coated with two layers is designed to be located between the cortex and skull to minimize the damage from the insertion (figure 2(*d*)). After the insertion, the platform is then mounted on the skull using dental cements to fix the probe in the head. Over time, the cerebrospinal fluid (CSF) that exists between the skull and cortex dissolves the 4%

sucrose gel and only the flexible segment remains as shown in figure 2(*e*). As a result, the inserted probe in the brain is no longer restrained by the position of the platform, but rather moves with the micro-motion of the brain. Therefore, using this proposed probe, the chronic neuron damage incurred by the friction between the probe and the brain due to the micro-motion of the brain can be reduced. Furthermore, the insertion segment is thinner (15 μm thick) than that of the previously reported flexible probes to further reduce the neuron damage during the insertion process. Therefore, the proposed structure can reduce neuron damage not only during the insertion process but also after implantation.

2.2. Material properties of the sucrose gel and polyimide

The flexible segment is mainly composed of a sucrose gel and a photosensitive polyimide film. To use these materials in the proposed flexible MEMS neural probe, characterization of both the dissolution time of the sucrose gel and flexibility of the polyimide film is important.

Sucrose is a biocompatible and biodegradable organic compound [43–48]. Sucrose gel is formed when 400 mg of the sucrose is mixed with 10 ml of the deionized water and can be completely dissolved in water within 1 h at room temperature. The sucrose gel is solidified in 10 min at 85 °C and Young's modulus of the solidified sucrose gel is 3.69 GPa. Furthermore, we can control the viscosity of the sucrose gel by adjusting the sucrose and deionized water ratio. Therefore, we can selectively coat the sucrose gel only on the flexible region of the proposed MEMS neural probe. Also, we can control the stiffness of the flexible segment by adjusting the thickness of the sucrose gel. In this work, we used the 4% sucrose gel to achieve appropriate viscosity and thickness for coating and insertion, respectively.

The flexible polyimide film has been widely used in various MEMS devices and biosensors because of its biocompatibility [49, 50]. Recently, photosensitive polyimides have been introduced which can be easily patterned using the standard photolithography process. Also, we can easily control the polyimide film thickness by adjusting the spin-coating speed and the viscosity of the photosensitive polyimide. Young's modulus, Poisson's ratio and density of the polyimide are 3.2 GPa, 0.34 and 1430 kg m^{-3}, respectively.

Based on these properties, both the polyimide and sucrose gels are good candidates for the flexible segment and thus both are used to form the flexible segment of the proposed MEMS neural probe.

2.3. Fabrication process

The proposed flexible MEMS neural probe was successfully fabricated using micromachining fabrication technology (figure 3). The fabrication process starts on a 4 inch SOI (silicon on insulator) wafer with top silicon thickness of 15 μm, buried oxide thickness of 0.7 μm and bottom silicon thickness of 500 μm (figure 3(*a*)). The thickness of the top silicon layer determines the thickness of the fabricated neural probe, and the buried oxide layer is used as an etch stop layer during the DRIE (deep reactive ion etching) process for the final release of

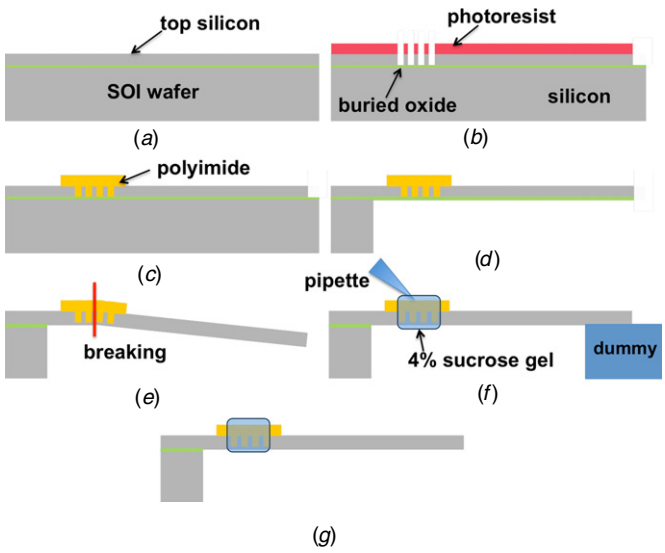

Figure 3. Fabrication process of the proposed flexible neural probe. (*a*) Starting with an SOI wafer. (*b*) Si DRIE etching using photoresist mask. (*c*) Patterning of 13 μm thick polyimide. (*d*) Release of the probe using silicon etching from backside using the DRIE process. (*e*) Breaking the flexible region. (*f*) Coating with 4% sucrose gel on the flexible segment with seating the end of the probe on the dummy structure.

the probe. First, easily breakable silicon region was patterned as a lattice structure by the deep silicon etching process. At the same time, the probe shape was defined; the 15 μm thick top silicon layer was patterned using photoresist and etched as shown in figure 3(*b*). Next, a photosensitive polyimide layer (HD4100, HD Microsystems) was spin-coated and patterned to complete the flexible segment. Then, the polyimide film was curried for 2 h in a convection oven at 200 °C. The thickness of the polyimide layer was measured to be approximately 13 μm. The width of the polyimide-patterned region (140 μm) is designed to be slightly wider than that of the probe (100 μm) to ensure full coverage of the polyimide layer over the flexible segment. In order to release the probe structure, we mounted the SOI wafer on a carrier using the Crystalbond™ (SPI Supplies, PA, USA) that is dissolved in hot water to avoid any process failure during the backside DRIE process. The 500 μm thick bottom silicon of the SOI wafer was removed by the DRIE process and 0.7 μm thick buried oxide layer was etched from the backside by the RIE etching process. During this process, a thick photoresist layer was used as an etch mask layer as shown in figure 3(*d*). After the release, the flexible segment consisting of the breakable silicon was broken to achieve the initial flexible status (figure 3(*e*)). Finally, a 4% sucrose gel was coated on the flexible region and cured for 10 min in an oven at 85 °C as shown in figure 3(*f*). For further characterization and *in vivo* experiments, the fabricated probes were mounted on a custom-designed printed circuit board.

3. Result and discussion

3.1. Fabrication result of the flexible MEMS probe

The SEM (scanning electron microscopy) images of the fabricated flexible probe composed of the insertion and flexible

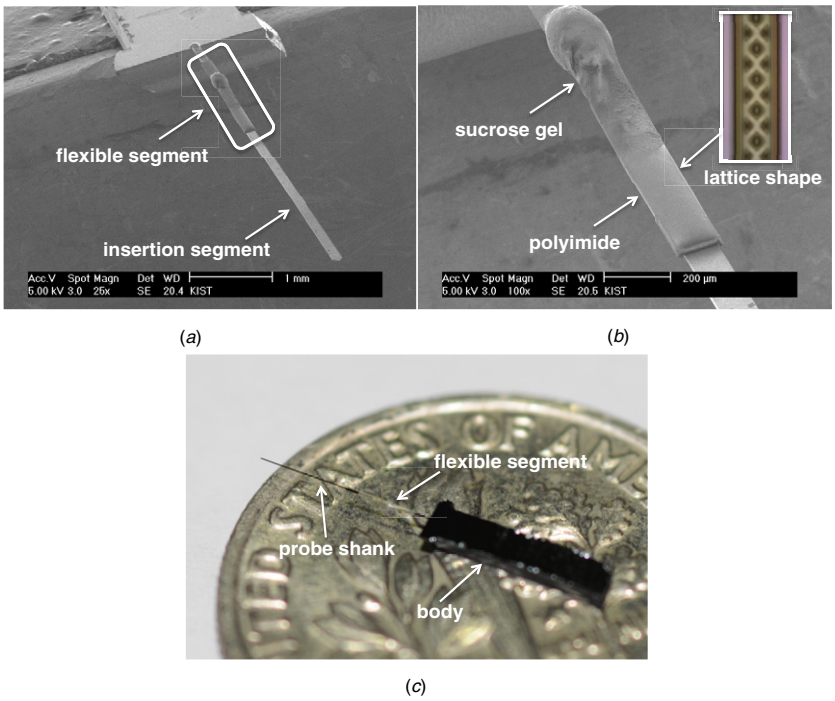

Figure 4. The SEM images and photo image of the fabricated flexible neural probe. (*a*) Fabricated flexible neural probe that is composed of the flexible segment and the insertion segment. (*b*) Flexible segment composed of lattice shape silicon and polyimide coated with 4% sucrose gel. (*c*) Fabricated flexible neural probe on a US Dime.

connection segments are shown in figures 4(*a*) and (*b*). The insertion segment consists of only a thin silicon layer (∼15 μm) to minimize neuron damage during the insertion process. In addition, the width of the insertion segment is 100 μm which is comparable to that of the conventional neural probe integrated with 16-electrodes [34]. The length of the insertion segment is 3.5 mm long to target the hippocampus region of a mouse brain. Also, the thickness of the insertion segment of the flexible probe is 15 μm to achieve sufficient stiffness for successful insertion without buckling. The probe tip is sharp with an angle of 45° for easy penetration where the insertion force is concentrated at the end of the probe.

The flexible segment consists of the silicon lattice structure covered with the polyimide and the 4% sucrose gel layer. Figure 4(*b*) shows that the polyimide layer completely covers the silicon lattice structure. The inset microscope images show the lattice pattern inside the polyimide and sucrose gels. In addition, the broken region is covered with the sucrose gel to ensure that this segment is flat and stiff enough for a successful insertion. The length and width of the lattice structure are 1 mm and 100 μm, respectively, where the width of the lattice patterns is 15 μm. The thickness of polyimide layer is approximately 13 μm which is strong enough to connect the insertion segment to the platform while the dimension is 2 mm × 140 μm (length × width) to fully cover the silicon lattice structure. Also, the thickness of the solidified sucrose gel is more than 100 μm, which does not induce any damage during the insertion process because this segment is designed to be located between the brain and skull. Figure 4(*c*) shows the fabricated 5.5 mm long flexible MEMS neural probe on a US dime to illustrate that the probe shank is straight.

3.2. Insertion force analysis

When the probe is inserted into a brain, the probe should penetrate the brain without buckling. The buckling can potentially lead to the breakage of the probe due to excessive bending. Therefore, it is important to design the neural probe with enough stiffness. The maximum brain tissue force is known to be 1000 μN [51] and thus, the maximum sustainable force of the neural probe without buckling should be larger than 1000 μN. In this proposed neural probe structure, there is a high chance of buckling phenomenon at the flexible segment and thus this segment should be designed to exhibit enough stiffness. One of the design parameters to enhance the stiffness of the flexible segment is the thickness of the sucrose gel.

To calculate the buckling force of the flexible segment, the thickness of the polyimide layer and sucrose gel should be calculated through equations (1) and (2). However, as shown in figure 4(*b*), the thickness of the sucrose gel is not uniform over the coated region. Therefore, the minimum thickness and width were used to calculate the buckling force. Young's modulus of polyimide is 3.2 GPa and the cross-sectional dimension of polyimide is 140 μm × 13 μm (width (*b*) × thickness (*h*)). Also, Young's modulus of sucrose is 3.69 GPa and the cross-sectional dimension of sucrose is 150 μm × 20 μm (width (*b*) × thickness (*h*)). The length of the polyimide and 4% sucrose gel was measured to be 2 mm. When the neural probe is inserted into a brain, the neural probe structure can be modeled as one-pined end and one-fixed end, where the effective length factor is 2.045. By using the obtained values, the buckling force can be calculated using the following equations:

$$P_{cr} = \frac{K \cdot \pi^2 \cdot E \cdot I}{L^2}, \tag{1}$$

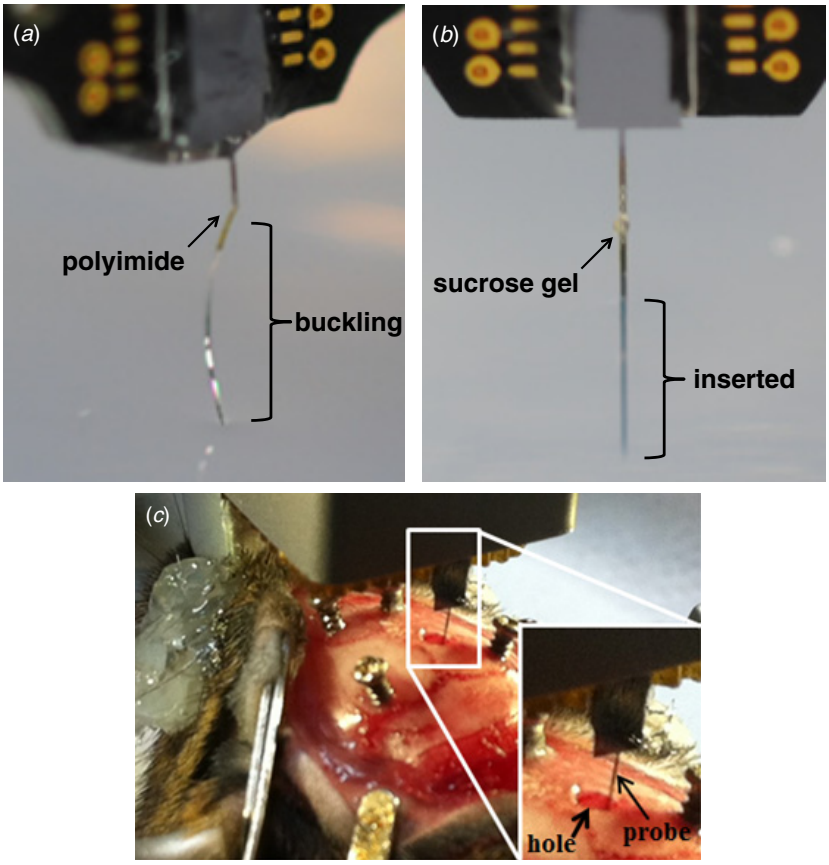

Figure 5. Insertion test of the fabricated flexible probe. (*a*) Insertion test of polyimideonly neural probe. (*b*) Insertion test of the neural probe coated with the sucrose gel on top of the polyimide layer. (*c*) Insertion of the fabricated flexible neural probe into a mouse brain for *in vivo* test during the five weeks.

$$I = \frac{1}{12} \cdot b \cdot h^3, \tag{2}$$

where, P_{cr} is the buckling force, K is the length factor, E is Young's modulus, L is the length of the flexible region, I is the moment of inertia, b is the width and h is the height of the flexible region.

The buckling force of only the polyimide at the flexible segment is calculated to be about 135 μN. However, the force is less than 1000 μN and thus the polyimide flexible segment cannot be inserted into a brain. In contrast, when the 20 μm thick 4% sucrose gel is coated on the flexible segment, the total buckling force at the flexible segment is calculated to be about 1736 μN, which is sufficiently larger than the tissue force of 1000 μN. Therefore, the neural probe coated with 4% sucrose gel in addition to the polyimide layer can exert sufficient force to be inserted into a brain. For the comparison, the bucking force of conventional 15 μm thick silicon probe is calculated to be 2900 μN, which is large enough to be inserted into a brain.

3.3. Insertion test of flexible neural probe

To test the insertion of the fabricated flexible neural probe, we prepared 0.6% agarose gel, which has similar rigidity to that of the brain [52]. To compare rigidity, two probes were prepared: one coated with only the polyimide and the other coated with the sucrose gel. In this experiment, the estimated thickness of the sucrose gel coated on the polyimide layer was approximately 100 μm. Both probes were inserted into 0.6% agarose gel as shown in figures 5(*a*) and (*b*). The probe coated with only the polyimide was buckled during the insertion, thus failed to penetrate the brain. In contrast, the flexible neural probe coated with the sucrose gel was successfully inserted into the 0.6% agarose gel without buckling as shown in figure 5(*b*). These results clearly confirm that the 100 μm thick 4% sucrose gel can mechanically support the flexible segment and prevents buckling during the insertion procedure. Also, the sucrose gel would maintain the rigidity until dissolved by the CSF in the brain. Accordingly, the insertion time would not be limited by the degradation time of a biodegradable polymer, while previously reported flexible neural probe coated with a biodegradable polymer over the entire probe is subject to time limit during the insertion procedure.

3.4. In vivo experiment and immunostaining

The proposed flexible neural probe is expected to incur less neuron damage during the insertion process and long-term chronic animal experiments. To compare the neuron damage induced by the proposed flexible neural probe with that by conventional neural probe, *in vivo* tests were performed with mice for five weeks using the conventional MEMS neural probe and the fabricated flexible neural probe. The dimensions

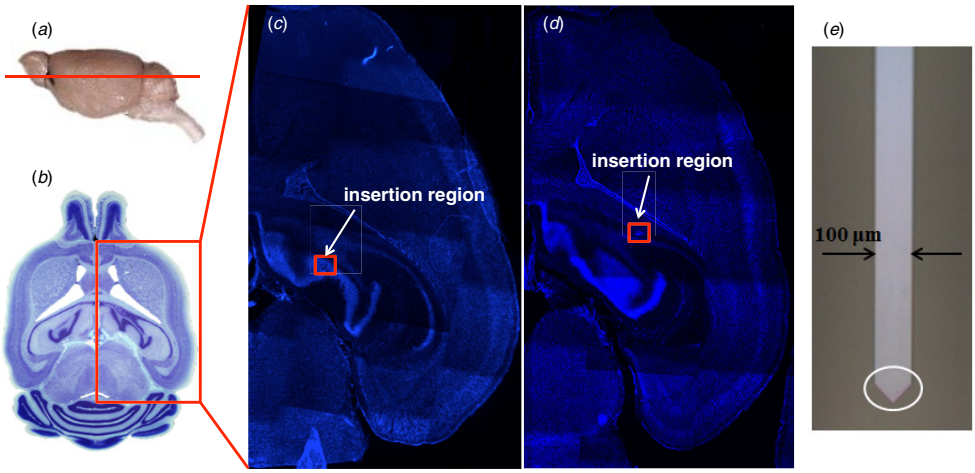

Figure 6. Sliced brain samples for damage comparison. (*a*) Photo image of the general mouse brain as seen from the side of the brain and the red line specifies the region of observation at a depth of 3.61 mm. (www.mbl.org). (*b*) Optical image of the horizontal brain atlas where the tip of the neural probe was located. (www.mbl.org). (*c*) Photo image of the brain slice showing the insertion region of the flexible probe. (*d*) Photo image of the brain slice showing the insertion region of the rigid probe. (*e*) Optical image of the insertion segment of the fabricated probe.

of two probes are identical where length, width and thickness are 5.5 mm, 100 μm and 15 μm, respectively. The conventional rigid MEMS probe is composed of a thin silicon layer (15 μm) and the fabricated flexible neural probe has a partially flexible connection segment as previously explained.

For an *in vivo* experiment, the skull of an anesthesia mouse was drilled to generate a 1 mm diameter hole. Through this hole, the probe was inserted 3.5 mm deep into the brain to the surface by penetrating dura mater. The flexible segment coated with the 4% sucrose gel was located between the cortex surface and the skull. The segment would be dissolved spontaneously after the insertion. After the surgery, the flexible probe was fixed on the head of the mouse by using biocompatible cement. To avoid any coverage of the flexible region by cement, we filled the hole with Vaseline and covered the region with cement. Vaseline is a biocompatible material [53] and also will be dissolved inside the brain by body temperature. The conventional rigid MEMS neural probe was also implanted into the brain of the other mouse under the same procedure. Then, mice were sacrificed on the fifth week from the implantation and brains were harvested and dissected in the frozen condition (50 μm thickness).

For immunostaining, brain tissue sections were fixed with 3.7% formaldehyde and permeablized with 0.1% Triton X-100 in PBS. Immunostaining with anti-mouse CD11b antibody (Abam Inc.) labels microphage/microglia induced by neuronal damage after the probe implantation [4, 54]. For the counter stain, Hoechst dye was used to identify nuclei in the brain section.

By using an optical microscope, we were able to trace the marks of the implanted MEMS neural probes and found that both probes were implanted down to the depth of 3.6 mm from the brain surface. Most of the MEMS neural probes consist of recording electrodes at the end of the probe for neural signal recording. Therefore, it is important to inspect neuron damages near the tip region where the neural probe inserted. Figure 6(*a*) shows an optical picture of the side of general mouse brain to obtain horizontal slices. The red line specifies the region of observation at a depth of 3.61 mm. Figure 6(*b*) shows the horizontal brain atlas where the tip of the neural probe was located. Blue dots show Hoechst stained nuclei for indicating the brain structure. Figures 6(*c*) and (*d*) show that the neural probes were implanted properly at the target position at a depth of 3.6 mm.

3.5. Neuron damage

The red boxes in figures 6(*c*) and (*d*) indicate the insertion regions of the probes, which illustrate that the probes were inserted near hippocampus where neuron density is high. Figure 6(*e*) shows an optical image of the fabricated probe, of which the width is smaller than 100 μm at the end of the probe. Therefore, the damaged region is expected to be comparable to the probe dimension.

Figures 7(*a*) and (*b*) show the bright field images of brain slices where the tips of probes were located. The yellow dotted line indicates the boundary of the damaged region. The damaged region induced by the rigid probe (figure 7(*a*)) is about five times larger than the damaged region induced by the flexible probe (figure 7(*b*)). The result was corresponding to the immunofluorescence stain of microglia/macrophage shown in figures 7(*c*) and (*d*). Both microglia and macrophages contribute to the immune response by acting as antigen presenting cells in the brain. Thus, when neurons are damaged by the foreign substances such as a neural probe, the microglia and macrophage are activated around the neural probe by the immune response known as the foreign body reaction. As shown in figures 7(*c*) and (*d*), macrophage and microglia that are stained with red color surround the implanted neural probe by the foreign body reaction, and thus we could measure the damaged region. Furthermore, the intensity of red color indicates the density of macrophage and microglia. Figures 7(*c*) and (*d*) demonstrate the damaged region by the rigid probe and the flexible probe, respectively. The border of

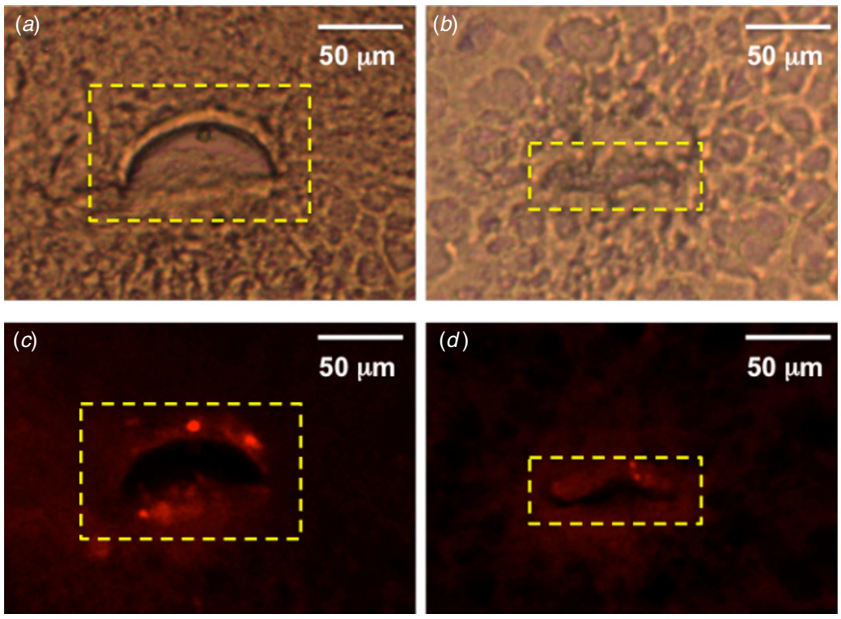

Figure 7. Immunostaining of two sliced brain samples for neural damage analysis. (*a*) Bright field image of the brain slice where the rigid probe was located. (*b*) Bright field image of the brain slice where the flexible probe was located. (*c*) Immunofluorescence stain of microglia/macrophage activated by the rigid probe with CD11b. (*d*) Immunofluorescence stain of microglia/macrophage activated by the flexible probe with CD11b.

the microglia and macrophage of the flexible probe is about five times smaller than that of the conventional rigid probe. Also, not only the intensity of red color is weaker but also the visible disruption in the surrounding tissue induced by the flexible probe is less evident. The bright field images and the immunofluorescence analysis of microglia/macrophage confirm that use of the flexible probe in fact reduces the neural damage compared to that caused by the use of the conventional rigid probe. The proposed flexible neural probe efficiently decreased cell death induced by mechanical stress from the implanted probe and greatly reduced immune responses. Thus, we believe that the proposed probe is a promising candidate for long-term chronic neural signal recording applications.

4. Conclusion

In this paper, we proposed and fabricated a flexible MEMS neural probe that composes of a partially flexible segment. The fabricated flexible neural probe has a thin insertion segment to reduce the brain damage during the insertion. In addition, the flexible segment can reduce the brain damage caused by the micro-motion of a brain because the insertion segment is no longer restrained by the platform and moves with brain. Therefore, the proposed probe can reduce the neural damage not only during the insertion process but also after the implantation. To maintain the rigidity of the flexible segment for successful insertion, a biodegradable sucrose gel is coated on the flexible segment, which is dissolved in the brain after the insertion. While the flexible probe is located in the brain, the flexible probe is mainly moved by the brain movement because the partially flexible polyimide segment is located between the cortex and skull.

In this paper, we demonstrated that neural damage induced by this flexible probe is about five times smaller than that induced by the conventional neural probe through immunostaining results obtained after five weeks of chronic implantation.

Furthermore, compared to the previously reported flexible neural probes, the proposed flexible MEMS neural probe has distinctive advantages. One of the advantages is that the neural damage region is smaller than that caused by other flexible probes because the thickness of the insertion segment of the flexible probe is thinner than other flexible probes coated with biodegradable materials over the entire probe region. In addition, the insertion time of the proposed flexible probe is not limited since the 4% sucrose gel coated on the partially flexible segment is not dissolved during the insertion period.

Therefore, the proposed flexible neural probe is a promising candidate for chronic neural signal recording applications. Future works include adding microelectrodes to the flexible probe and recording neural signals over a long period of time.

Acknowledgments

This work was partially supported by KIST Institutional Program (2E23880) and the National Research Foundation (NRF) grant funded by the Korea Government (MEST) (no. 2012R1A2A2A02118 38).

References

[1] Hodgkin A L and Huxley A F 1952 A quantitative description of membrane current and its application to conduction and excitation in nerve *J. Physiol.* **117** 500–44
[2] Wise K D 2005 Silicon microsystems for neuroscience and neural prostheses *IEEE Eng. Med. Biol. Mag.* **24** 22–29
[3] Schwartz A B 2004 Cortical neural prosthetics *Annu. Rev. Neurosci.* **27** 487–507

[4] Szarowski D H *et al* 2003 Brain responses to micro-machined silicon devices *Brain Res.* **983** 23–35

[5] HajjHassan M, Chodavarapu V and Musallam S 2008 NeuroMEMS: neural probe microtechnologies *IEEE Sensors J.* **8** 6704–26

[6] Robinson D A 1968 The electrical properties of metal microelectrodes *Proc. IEEE* **56** 1065–71

[7] Skrzypek J and Keller E 1975 Manufacture of metal microelectrodes with the scanning electron microscope *IEEE Trans. Biomed. Eng.* **22** 435–7

[8] Nicolelis M A 2003 Brain–machine interfaces to restore motor function and probe neural circuits *Nature Rev. Neurosci.* **4** 417–22

[9] Rutten W L 2002 Selective electrical interfaces with the nervous system *Annu. Rev. Biomed. Eng.* **4** 407–52

[10] Benabid A L, Chabardes S, Mitrofanis J and Pollak P 2009 Deep brain stimulation of the subthalamic nucleus for the treatment of Parkinson's disease *Lancet Neurol.* **8** 67–81

[11] Zhang M, Kibler A and Durand D M 2011 Mapping 4-AP induced epilepsy propagation with a micro-electrode array in intact hippocampus *in-vitro 5th Int. IEEE/EMBS Conf. on Neural Eng.* pp 621–4

[12] Hubel D H 1957 Tungsten microelectrode for recording from single units *Science* **125** 549–50

[13] Newman R and Ajjawi M 1986 A micro-electrode study of the nitrate effect on pitting of stainless steels *Corros. Sci.* **26** 1057–63

[14] Battaglia F P *et al* 2009 The Lantern: an ultra-light micro-drive for multi-tetrode recordings in mice and other small animals *J. Neurosci. Methods* **178** 291–300

[15] Buzsáki G and Draguhn A 2004 Neuronal oscillations in cortical networks *Science* **304** 1926–9

[16] Varela F, Lachaux J-P, Rodriguez E and Martinerie J 2001 The brainweb: phase synchronization and large-scale integration *Nature Rev. Neurosci.* **2** 229–39

[17] Brown E N, Kass R E and Mitra P P 2004 Multiple neural spike train data analysis: state-of-the-art and future challenges *Nature Neurosci.* **7** 456–61

[18] Norlin P, Kindlundh M, Mouroux A, Yoshida K and Hofmann U G 2002 A 32-site neural recording probe fabricated by DRIE of SOI substrates *J. Micromech. Microeng.* **12** 414–9

[19] Wise K D 2007 Integrated sensors, MEMS, and microsystems: reflections on a fantastic voyage *Sensors Actuators* A **136** 39–50

[20] Wise K D, Sodagar A M, Yao Y, Gulari M N, Perlin G E and Najafi K 2008 Microelectrodes, microelectronics, and implantable neural microsystems *Proc. IEEE* **96** 1184–202

[21] Wise K D 2005 Silicon microsystems for neuroscience and neural prostheses *IEEE Eng. Med. Biol. Mag.* **24** 22–29

[22] Ruther P, Herwik S, Kisban S, Seidl K and Paul O 2010 Recent progress in neural probes using silicon MEMS technology *IEEJ Trans. Electr. Electron. Eng.* **5** 505–15

[23] Kisban S *et al* 2007 Microprobe array with low impedance electrodes and highly flexible polyimide cables for acute neural recording *EMBS'07: Proc. 29th IEEE Int. Conf. on Engineering in Medicine and Biological Society* pp 175–8

[24] John J, Li Y, Zhang J, Loeb J A and Xu Y 2011 Microfabrication of 3D neural probes with combined electrical and chemical interfaces *J. Micromech. Microeng.* **21** 105011

[25] Papageorgiou D P, Shore S E, Bledsoe S C and Wise K D 2006 A shuttered neural probe with on-chip flowmeters for chronic *in vivo* drug delivery *J. Microelectromech. Syst.* **15** 1025–33

[26] Yao Y, Gulari M N, Hetke J F and Wise K D 2003 A self-testing multiplexed CMOS stimulating probe for a 1024-site neural prosthesis *TRANSDUCERS: 12th Int. Conf. on Solid-State Sensors, Actuators and Microsystems (Technical Digest)* pp 1213–6

[27] Chen J K and Wise K D 1997 A silicon probe with integrated microheaters for thermal marking and monitoring of neural tissue *IEEE Trans. Biomed. Eng.* **44** 770–4

[28] Chen J K, Wise K D, Hetke J F and Bledsoe S C 1997 A multichannel neural probe for selective chemical delivery at the cellular level *IEEE Trans. Biomed. Eng.* **44** 760–9

[29] Kim C and Wise K D 1996 A 64-site multishank CMOS low-profile neural stimulating probe *IEEE J. Solid-State Circuits* **31** 1230–8

[30] Santhanam G, Ryu S I, Yu B M, Afshar A and Shenoy K V 2006 A high-performance brain–computer interface *Nature* **442** 195–8

[31] Rousche P J and Normann R A 1998 Chronic recording capability of the Utah intracortical electrode array in cat sensory cortex *J. Neurosci. Methods* **82** 1–15

[32] Maynard E M, Nordhausen C T and Normann R A 1997 The Utah intracortical electrode array: a recording structure for potential brain–computer interfaces *Electroencephalogr. Clin. Neurophysiol.* **102** 228–39

[33] Kelly R C *et al* 2007 Comparison of recordings from microelectrode arrays and single electrodes in the visual cortex *J. Neurosci.* **27** 261–4

[34] Cho I-J, Baac H W and Yoon E 2010 A 16-site neural probe integrated with a waveguide for optical stimulation *MEMS: Proc. 23rd IEEE Int. Conf. on Micro Electro Mechanical Systems* pp 995–8

[35] Zorzos A N, Boyden E S and Fonstad C G 2010 Multiwaveguide implantable probe for light delivery to sets of distributed brain targets *Opt. Lett.* **35** 4133–5

[36] Polikov V S, Block M L, Fellous J M, Hong J S and Reichert W M 2006 *In vitro* model of glial scarring around neuroelectrodes chronically implanted in the CNS *Biomaterials* **27** 5368–76

[37] Takeuchi S, Ziegler D, Yoshida Y, Mabuchi K and Suzuki T 2005 Parylene flexible neural probes integrated with microfluidic channels *Lab Chip* **5** 519–23

[38] Polikov V S, Tresco P A and Reichert W M 2005 Response of brain tissue to chronically implanted neural electrodes *J. Neurosci. Methods* **148** 1–18

[39] Seymour J P and Kipke D R 2007 Neural probe design for reduced tissue encapsulation in CNS *Biomaterials* **28** 3594–607

[40] Suzuki T, Mabuchi K and Takeuchi S 2003 A 3D flexible parylene probe array for multichannel neural recording *Proc. 1st IEEE Int. Conf. on Neural Engineering* pp 154–6

[41] Wu F, Im M and Yoon E 2011 A flexible fish-bone-shaped neural probe strengthened by biodegradable silk coating for enhanced biocompatibility *TRANSDUCERS: 16th Int. Conf. on Solid-State Sensors, Actuators and Microsystems (Technical Digest)* pp 966–9

[42] Gilgunn P *et al* 2012 An ultra-compliant, scalable neural probe with molded biodissolvable delivery vehicle *MEMS: Proc. 25th IEEE Int. Conf. on Micro Electro Mechanical Systems* pp 56–59

[43] Ferreira L, Vidal M, Geraldes C and Gil M 2000 Preparation and characterisation of gels based on sucrose modified with glycidyl methacrylate *Carbohydr. Polym.* **41** 15–24

[44] Lee J *et al* 2006 Intracranial drug-delivery scaffolds: biocompatibility evaluation of sucrose acetate isobutyrate gels *Toxicol. Appl. Pharmacol.* **215** 64–70

[45] Vermeire A, Muynck C, Vandenbossche G, Eechaute W, Geerts M L and Remon J P 1996 Sucrose laurate gels as a percutaneous delivery system for oestradiol in rabbits *J. Pharm. Pharmacol.* **48** 463–7

[46] Miller J S *et al* 2012 Rapid casting of patterned vascular networks for perfusable engineered three-dimensional tissues *Nature Mater.* **11** 768–74

[47] Van Sliedregt A, Van Loon J A, Van Der Brink J, De Groot K and Van Blitterswijk C A 1994 Evaluation of polylactide monomers in an *in vitro* biocompatibility assay *Biomaterials* **15** 251–6

[48] Guse C, Koennings S, Kreye F, Siepmann F, Göpferich A and Siepmann J 2006 Drug release from lipid-based implants: elucidation of the underlying mass transport mechanisms *Int. J. Pharm.* **314** 137–44

[49] Rousche P J, Pellinen D S, Pivin D P Jr, Williams J C and Vetter R J 2001 Flexible polyimide-based intracortical electrode arrays with bioactive capability *IEEE Trans. Biomed. Eng.* **48** 361–71

[50] Seo J-M, Kim S J, Chung H, Kim E T, Yu H G and Yu Y S 2004 Biocompatibility of polyimide microelectrode array for retinal stimulation *Mater. Sci. Eng.* C **24** 185–9

[51] Wester B A, Lee R H and LaPlaca M C 2009 Development and characterization of *in vivo* flexible electrodes compatible with large tissue displacements *J. Neural Eng.* **6** 024002

[52] Hall T J, Bilgen M, Insana M F and Krouskop T A 1997 Phantom materials for elastography *IEEE Trans. Ultrason. Ferroelectr. Freq. Control* **44** 1355–65

[53] Kubie J L 1984 A driveable bundle of microwires for collecting single-unit data from freely-moving rats *Physiol. Behav.* **32** 115–8

[54] Mercanzini A *et al* 2008 Demonstration of cortical recording using novel flexible polymer neural probes *Sensors Actuators* A **143** 90–96